Satellite Phase and Code Bias Estimation with Cascaded Kalman Filter

Z. Wen*, P. Henkel*, M. Davaine* and C. Günther*,**
*Technische Universität München (TUM), Munich, Germany
**German Aerospace Center (DLR), Oberpfaffenhofen, Germany

BIOGRAPHIES

Zhibo Wen received his master degree in electrical engineering and information technology from the Technische Universität München, Germany, with the rating passed high distinction. He has received the "Leo-Brandt-Preis - DGON Master of Navigation" from the German Institute of Navigation for his master thesis on estimation of code and phase bias in satellite navigation. During his master studies, he has received a DAAD scholarship and an MAN scholarship for his excellent grades. He is currently a PhD candidate at the Institute for Communications and Navigation, Technische Universität München, working on precise point positioning.

Patrick Henkel studied electrical engineering and information technology at the Technische Universität München, Munich, Germany, and the École Polytechnique de Montréal, Canada. He then started his PhD on reliable carrier phase positioning and graduated in 2010 with "summa cum laude". He is now working towards his habilitation in the field of precise point positioning. He was a guest researcher at TU Delft in 2007, and at the GPS Lab at Stanford University, Stanford, in 2008 and 2010. Patrick received the Pierre Contensou Gold Medal at the Intern. Astronautical Congress in 2007, the Bavarian regional prize at the European Satellite Navigation Competition in 2010, and the "Vodafone Förderpreis" for his dissertation in 2011. He is also one of the founders of Advanced Navigation Solutions - AMCONAV GmbH.

Mathieu Davaine has joined the double degree program from Technische Universität Müchen and the French grande école Supélec in Gif sur Yvette. He studied electrical engineering and information technology during his master program. He has written his master thesis on "Code Bias and Multipath Estimation with Cascaded Kalman Filter" at the Institute for Communications and Navigation, Technische Universität München.

Christoph Günther studied theoretical physics at the Swiss Federal Institute of Technology in Zurich. He received his diploma in 1979 and completed his PhD in 1984. He worked on communication and information theory at Brown Boveri and Ascom Tech. From 1995, he led the development of mobile phones for GSM and later dual mode GSM/Satellite phones at Ascom. In 1999, he became head of the research department of Ericsson in Nuremberg. Since 2003, he is the director of the Institute of Communication and Navigation at the German Aerospace Center (DLR) and since December 2004, he additionally holds a Chair at the Technische Universität München (TUM). His research interests are in satellite navigation, communication and signal processing.

ABSTRACT

This paper suggests a new method for the estimation of satellite phase and code biases with undifferenced, uncombined phase and pseudorange measurements from a global network of reference stations. The method is based on a generalized measurement model with individual phase and pseudorange biases for each satellite, and uses a generalized Kalman filter for coloured measurement noise.

The estimation of phase and code biases is performed with a cascade of two Kalman filters: First, the non-dispersive parameters of each receiver-satellite link are combined into a single geometry term, and a conventional Kalman filter is used to estimate the geometry term, ionospheric delays, and individual ambiguities. The mapping of all non-dispersive parameters to single geometry terms improves the conditioning of the system of equations and, thereby, enables a faster ambiguity fixing. A second filter is then used to refine the geometry term, i.e. to estimate orbital errors, code biases and tropospheric delays. As the a posteriori estimates of the first Kalman filter are correlated over time and correspond to the measurement of the second filter, the generalized Kalman filter of Bryson and Henrikson is used to whiten the measurement noise and to keep the measurement and process noises independent.

One of the largest challenges for reliable precise point

positioning with integer ambiguity resolution is code multipath, which has to be considered carefully at both the reference stations and mobile receiver. For the reference station, a sidereal filtering can be applied to the pseudorange residuals to efficiently obtain multipath corrections. It is shown that these corrections whiten the measurement noise and result in substantially improved stability of the bias estimates.

INTRODUCTION

Double-differencing enables integer ambiguity fixing and positioning with millimeter-level accuracy, since it removes most of the common errors, such as the ionospheric and tropospheric delays and satellite biases with the help of a nearby reference station. Meanwhile, absolute precise point positioning is becoming increasingly popular as it provides centimeter-level accuracy without the need of a reference station. However, resolving the undifferenced carrier phase integer ambiguities requires precise estimates of the satellite code and phase biases [1–4].

Recently, Laurichesse et al. [5–7] have shown that fractional widelane biases can be assumed constant over several months and narrowlane biases are still constant on a daily basis, which enabled them to demonstrate undifferenced integer ambiguity resolution. They used a two steps procedure, where widelane fractional biases and integer ambiguities are first obtained from the geometry-free, ionosphere-free Melbourne Wübbena combination [8]. In a second step, the phase measurements are combined to ionosphere-free combinations, which are then processed in an extended Kalman filter to estimate ionosphere-free phase clocks of both satellites and receivers, offsets between ionosphere-free phase and pseudorange clocks, zenith tropospheric delays, station coordinate corrections, satellite orbit corrections, and L1 phase ambiguities. The fractional widelane biases from the first step, the orbital errors, the ionosphere-free phase clocks as well as the offsets between phase and pseudorange clocks from the second step form the four correction parameters, which Laurichesse suggested for precise point positioning.

Code multipath is one of the most challenging error sources for precise point positioning. The multipath estimation from the reference station can be observed from the repeatability of range residuals at equal receiver-satellite geometries, and can be precisely estimated by sidereal filtering. In the first part of this paper, pseudorange residuals are analyzed both in time and frequency domain, and a multipath correction is computed which whitens the measurement noise and results in a two times lower standard deviation. The second part focuses on the satellite code bias estimation based on a very general measurement model, which does not use any combinations of measurements. The bias estimation is performed with a cascaded Kalman filter, where a first Kalman filter is used to estimate the geometry terms (including all non-dispersive parameters), the ionospheric delays, the integer ambiguities and the phase biases. A second stage Kalman filter uses the geometry estimates from the first stage as new measurements to estimate satellite orbit corrections, satellite code biases and receiver clock offsets. As the first filtering introduces some time correlation into the geometry estimates, the method of Bryson and Henrikson [9,10] is applied to decorrelate the measurements by a pre-processing. Simulation results indicate that both code multipath corrections and the cascaded Kalman filter are two important steps to improve the reliability of precise point positioning.

MEASUREMENT MODEL

In the approach of Wen et al. [1] [3], Henkel et al. [2], and Davaine [4], the absolute code and phase measurements on two frequencies are modeled as

$$\begin{aligned}
\lambda_1\phi_{1,i}^k(t_n) &= \tilde{g}_i^k(t_n) - \tilde{I}_{1,i}^k(t_n) + \lambda_1\tilde{N}_{1,i}^k + \\
&\qquad \tilde{\tilde{\tilde{\beta}}}_{1,i} + \tilde{\tilde{\tilde{\beta}}}_1^k + \epsilon_{1,i}^k(t_n)\\
\lambda_2\phi_{2,i}^k(t_n) &= \tilde{g}_i^k(t_n) - q_{12}^2\tilde{I}_{1,i}^k(t_n) + \lambda_2\tilde{N}_{2,i}^k + \\
&\qquad \tilde{\tilde{\tilde{\beta}}}_{2,i} + \tilde{\tilde{\tilde{\beta}}}_2^k + \epsilon_{2,i}^k(t_n)\\
\rho_{1,i}^k(t_n) &= \tilde{g}_i^k(t_n) + \tilde{I}_{1,i}^k(t_n) + o_{1,i}^k(t_n) + \eta_{1,i}^k(t_n)\\
\rho_{2,i}^k(t_n) &= \tilde{g}_i^k(t_n) + q_{12}^2\tilde{I}_{1,i}^k(t_n) + o_{2,i}^k(t_n) + \eta_{2,i}^k(t_n),
\end{aligned} \tag{1}$$

with i, m and k representing receiver, frequency and satellite indices, λ_m being the wavelength, $q_{12} = f_1/f_2$ being the frequency ratio, $\tilde{I}_{1,i}^k$ denoting the ionospheric slant delay, $\tilde{N}_{m,i}^k$ being the integer ambiguity, $\{\tilde{\tilde{\tilde{\beta}}}_{m,i}, \tilde{\tilde{\tilde{\beta}}}_m^k\}$ being the phase biases, $o_{m,i}^k$ being the code multipath, and $\epsilon_{m,i}^k$ and $\eta_{m,i}^k$ being respectively the phase and code noise. The geometry term $\tilde{g}_i^k$ contains the non-frequency dependent terms and is described by

$$\begin{aligned}
\tilde{g}_i^k(t_n) &= r_i^k(t_n) + c(\delta\tau_i(t_n) - \delta\tau^k(t_n - \Delta\tau_i^k(t_n))) + \\
&\qquad T_i^k(t_n) + b_{g_i} + b_g^k,
\end{aligned} \tag{2}$$

where r_i^k denotes the true range, $c\delta\tau_i$ denotes the receiver clock offset, $c\delta\tau^k$ denotes the satellite clock offset, $\Delta\tau_i^k$ represents the propagation time from the satellite to the receiver, T_i^k denotes the tropospheric delay, b_{g_i} and b_g^k denote respectively the receiver and satellite code bias.

The tildes on the variables of Eq. (1) arise from a set of parameter mappings, which ensure a full-rank equation system, i.e. the code biases have been mapped to geometry and ionospheric terms, the satellite phase biases from one satellite have been mapped to the receiver phase biases and a subset of ambiguities is mapped to other ambiguities and phase biases.

MULTIPATH ESTIMATION

The estimation of multipath delays is in general not feasible in real-time, as multipath affects each satellite and frequency differently, and thus, the system of equations becomes rank deficient. However, multipath errors repeat with the satellite geometry, i.e. every $11\text{h}\ 58\text{mins}$ for geodetic reference stations. This allows a separation from all other error terms, and makes it well observable from the repeatability of the residuals. The latter ones are obtained from a Kalman filter, which estimates the joint geometry terms, the ionospheric delays, phase biases and integer ambiguities, where the ambiguities are considered as float numbers.

GPS measurements were collected from a few SAPOS stations in Bavaria [11] in the week between May 30 and June 5, 2011. In Fig. 1, the residuals of the SAPOS (Satellitenpositionierungsdienst der deutschen Landesvermessung) station at Günzburg (#274 in network) are shown for a GPS satellite (PRN 5) over 7 consecutive days. The period was 08:00 to 09:40 on the last day, and then shifted by 3mins 56s every day to take the repeatability of the satellite geometry into account. For clarity, the residuals were shifted in Fig. 1 by 2 meters in vertical directions to improve the visibility.

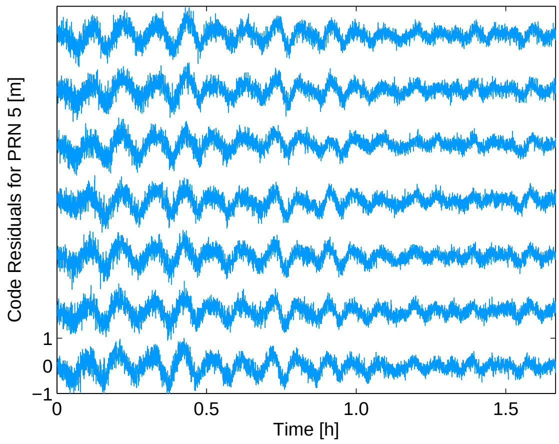

Fig. 1 Code residuals from SAPOS station at Günzburg on six consecutive days: A high repeatability can be observed over the days, which can be explained by multipath errors that repeat with the satellite geometry. Note that the residuals were artificially shifted in vertical direction to improve the visibility of the repeatability.

Fig. 2 shows the estimated code multipath at the station of Günzburg, which is obtained from a sidereal filtering of the code residuals over a continuous week. This average can then be used as a priori correction of multipath for the measurements on the next days.

Fig. 3 shows the benefit of the multipath correction, i.e. the correction derived from the measurements between May 30 and June 5 is applied to measurements on June 6.

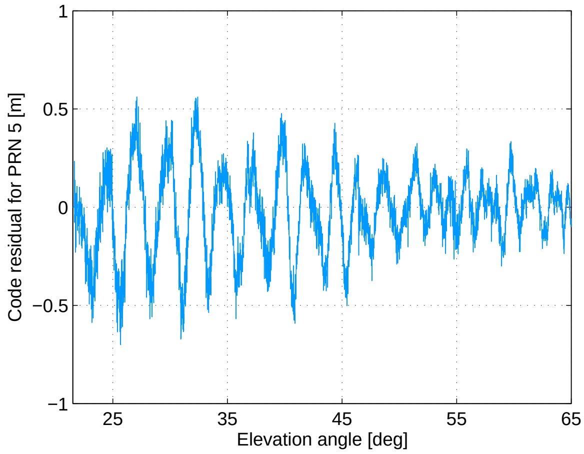

Fig. 2 Sidereal filtered code residuals of SAPOS station Günzburg over one week: The filtering substantially reduces the noise, which allows an accurate modeling of the multipath pattern.

One can observe that the new residuals are white Gaussian noise, i.e. the strong multipath pattern was removed.

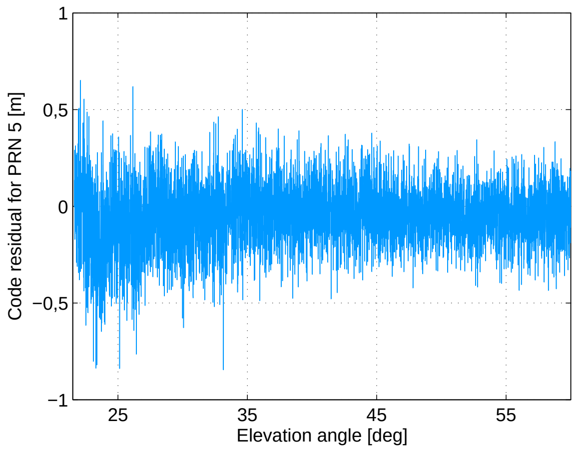

Fig. 3 Benefit of multipath correction: The correction removes the strong multipath pattern and results in a white Gaussian noise.

A histogram of the code residuals without and with application of the multipath correction is given in Fig. 4. It well approximates a bell-shape of a Gaussian distribution in both cases, while the red curve (representing the code residuals after applying the correction) concentrates more in the center. Consequently, the multipath correction enables the bounding of the measurement noise by a Gaussian distribution with significantly lower standard deviation.

The satellite phase bias estimation also benefits from the a priori knowledge of the multipath. A comparison of Fig. 5(a) and (b) shows that the oscillations of the bias estimates are suppressed, and a more smooth convergence is ensured.

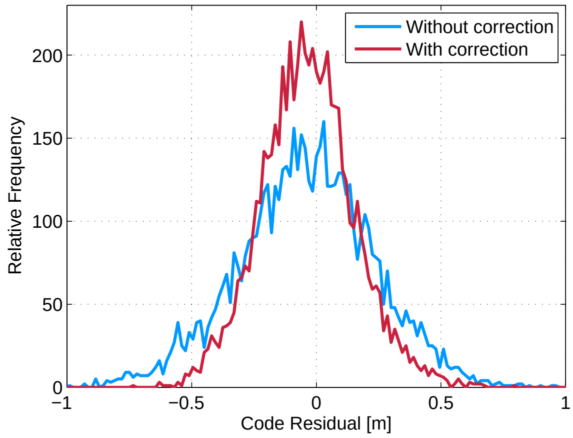

Fig. 4 Histogram of the code residuals without and with applying the multipath correction: The multipath correction results in a Gaussian distribution with significantly reduced standard deviation.

Moreover, the correction of multipath also helps for the integer ambiguity fixing, since the stability of the phase bias estimates has strong influence on the convergence of the ambiguities. Each vertical black line in both figures represents one ambiguity fixing. Without the correction of multipath, only 2 out of 90 ambiguities are fixed, while 40 ambiguities have been fixed in Fig. 5(b). One can also observe that the fixing of the first ambiguity takes place much earlier with the a priori information.

DUAL-STAGE KALMAN FILTER

Generalized Kalman Filter for colored measurements

The measurement and state space models of a conventional Kalman filter are given by

$$\begin{aligned} x_n &= \Phi_{n-1} x_{n-1} + w_{n-1} \\ z_n &= H_n x_n + \zeta_n, \end{aligned} \tag{3}$$

where x_n and z_n are the state and measurement vectors on epoch n, Φ_n is the state transition matrix, H_n is the geometry matrix, and w_n and ζ_n are the state and measurement noises, which follow zero mean Gaussian distributions with covariance

$$E(w_k w_l^{\mathrm{T}}) = Q_k \delta_{kl},\ E(\zeta_k \zeta_l^{\mathrm{T}}) = R_k \delta_{kl}, \tag{4}$$

with δ_{kl} being the Kronecker delta function. There is no correlation between state and measurement noises, i.e. $E(w_k \zeta_l^{\mathrm{T}}) = 0$.

For a cascading of Kalman filters, the assumptions of white measurement noise holds only in the first cascade. In all following cascades, the measurement noises are colored due to previous filtering processes.

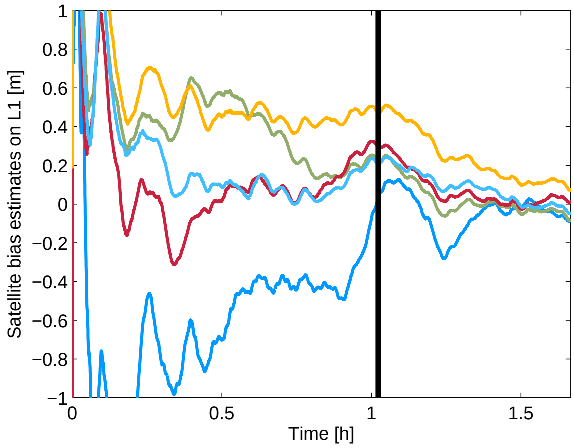

(a) No multipath correction

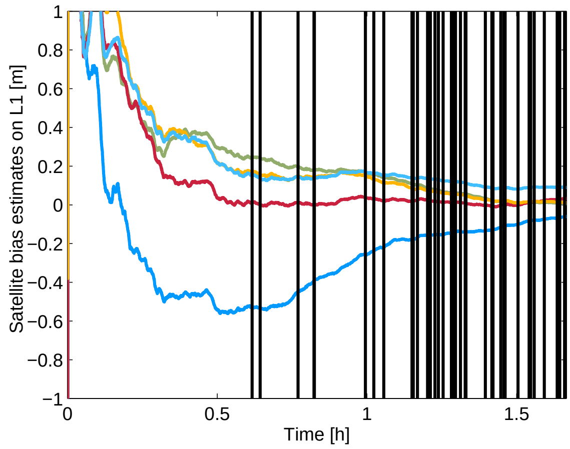

(b) With multipath correction

Fig. 5 Satellite bias estimation without and with multipath correction: The multipath error propagates into the bias estimates which show large variations over time and prevent a fast ambiguity fixing. In this case, only 2 out of 90 ambiguities have been fixed, which are indicated as vertical black lines. The multipath correction improves the stability of the phase bias estimates. The integer ambiguity fixings also benefit from the correction, i.e. the fixings occur much earlier and the number of fixings increases from 2 to 40.

This motivates more general measurement and state models, i.e.

$$\begin{aligned} x_n &= \Phi_{n-1} x_{n-1} + w_{n-1} \\ z_n &= H_n x_n + v_n \\ v_n &= \Gamma_{n-1} v_{n-1} + \zeta_{n-1}, \end{aligned} \tag{5}$$

where the matrix Γ_n describes the linear dependency of the measurement noise v_n between consecutive epochs, and w_n and ζ_n are independent white Gaussian noises, i.e.

$$E(w_n) = 0,\ E(w_n w_m^{\mathrm{T}}) = Q_n \delta_{nm}, \tag{6}$$

and

$$E(\zeta_n) = 0,\ E(\zeta_n \zeta_m^{\mathrm{T}}) = R_n \delta_{nm}$$
$$E(w_n \zeta_m^{\mathrm{T}}) = 0. \tag{7}$$

At first glance, one might augment the state vector by v_n and, thereby, return to white Gaussian measurement noise. However, this will introduce some linear dependency between the states and, thereby, results in a singularity. Therefore, Bryson and Henrikson suggested an alternative approach in [9]: It starts with a time "pseudo-differenced" measurement z_n^*, which eliminates the term $\Gamma_n v_n$ and only keeps the white Gaussian noises w_n and ζ_n, i.e.

$$\begin{aligned} z_n^* &= z_{n+1} - \Gamma_n z_n \\ &= H_{n+1} x_{n+1} + v_{n+1} - \Gamma_n \left(H_n x_n + v_n\right) \\ &= H_{n+1} \left(\Phi_n x_n + w_n\right) + \Gamma_n v_n + \zeta_n \\ &\quad - \left(\Gamma_n H_n x_n + v_n\right) \\ &= \left(H_{n+1} \Phi_n - \Gamma_n H_n\right) x_n + H_{n+1} w_n + \zeta_n \\ &= H_n^* x_n + v_n^*, \end{aligned} \tag{8}$$

with

$$\begin{aligned} H_n^* &\triangleq H_{n+1} \Phi_n - \Gamma_n H_n \\ v_n^* &\triangleq H_{n+1} w_n + \zeta_n. \end{aligned} \tag{9}$$

The new measurement noise v_n^* has therefore zero mean, and a covariance matrix R_n^* obtained from

$$\begin{aligned} E\{v_n^* v_m^{*\mathrm{T}}\} &= E\{(H_{n+1} w_n + \zeta_n) \left(H_{m+1} w_m + \zeta_m\right)^{\mathrm{T}}\} \\ &= \left(H_{n+1} Q_n H_{n+1}^{\mathrm{T}} + R_n\right) \delta_{nm} \\ &= R_n^* \delta_{nm}, \end{aligned} \tag{10}$$

with

$$R_n^* \triangleq H_{n+1} Q_n H_{n+1}^{\mathrm{T}} + R_n. \tag{11}$$

It can be observed from Eq. (9) that a correlation is introduced between the transformed measurement noise v_n^* and the process noise w_n, i.e.

$$\begin{aligned} E\{w_n v_m^{*\mathrm{T}}\} &= E\{w_n \left(H_{m+1} w_m + \zeta_m\right)^{\mathrm{T}}\} \\ &= \left(Q_n H_{n+1}^{\mathrm{T}}\right) \delta_{nm} \\ &= S_n \delta_{nm}, \end{aligned} \tag{12}$$

with

$$S_n \triangleq Q_n H_{n+1}. \tag{13}$$

Therefore, a decoupling between the two noises is necessary. It can be performed by introducing a new process noise w_n^*, which satisfies

$$\begin{aligned} E\{w_n^*\} &= 0 \\ E\{w_n^* w_m^{*\mathrm{T}}\} &= Q_n^* \delta_{nm} \\ E\{w_n^* v_m^{*\mathrm{T}}\} &= 0. \end{aligned} \tag{14}$$

The state transition in Eq. (5) can be rewritten by adding the transformed measurements as a zero term, i.e.

$$\begin{aligned} x_n &= \Phi_{n-1} x_{n-1} + w_n \\ &\quad + J_{n-1} \cdot \left(z_{n-1}^* - H_{n-1}^* x_{n-1} - v_{n-1}^*\right) \\ &= \Phi_{n-1}^* x_{n-1} + w_n^* + J_{n-1} z_{n-1}^*, \end{aligned} \tag{15}$$

where J_{n-1} is some weighting being introduced a few lines later, and Φ_n^* and w_n^* are defined as

$$\begin{aligned} \Phi_n^* &\triangleq \Phi_n - J_n H_n^* \\ w_n^* &\triangleq w_n - J_{n-1} v_{n-1}^*. \end{aligned} \tag{16}$$

The J_n matrix shall be chosen such that the new process noise is uncorrelated with the new measurement noise, i.e.

$$\begin{aligned} E\{w_n^* v_m^{*\mathrm{T}}\} &= E\{(w_n - J_n v_n^*) \, v_m^{*\mathrm{T}}\} \\ &= \left(S_n - J_n R_n^*\right) \delta_{nm} \\ &\stackrel{!}{=} 0, \end{aligned} \tag{17}$$

which can be easily solved for J_n:

$$J_n = S_n \left(R_n^*\right)^{-1}. \tag{18}$$

The optimized J_n can then be used to rewrite Q_n^* as

$$\begin{aligned} Q_n^* &= E\{w_n^* w_n^{*\mathrm{T}}\} \\ &= E\{(w_n - J_n v_n^*)(w_n - J_n v_n^*)^{\mathrm{T}}\} \\ &= E\{(w_n - S_n (R_n^*)^{-1} v_n^*)(w_n - S_n (R_n^*)^{-1} v_n^*)^{\mathrm{T}}\} \\ &= Q_n - S_n (R_n^*)^{-1} S_n^{\mathrm{T}} - S_n ((R_n^*)^{-1})^{\mathrm{T}} S_n^{\mathrm{T}} + \\ &\quad S_n (R_n^*)^{-1} R_n^* ((R_n^*)^{-1})^{\mathrm{T}} S_n^{\mathrm{T}} \\ &= Q_n - S_n (R_n^*)^{-1} S_n^{\mathrm{T}}. \end{aligned} \tag{19}$$

Combining Eq. (8), (9), (11), (13), (16), (18), and (19), the set of the new variables can be summarized as

$$\begin{aligned} z_n^* &= z_{n+1} - \Gamma_n z_n \\ H_n^* &= H_{n+1} \Phi_n - \Gamma_n H_n \\ S_n &= Q_n H_{n+1}^{\mathrm{T}} \\ R_n^* &= H_{n+1} Q_n H_{n+1}^{\mathrm{T}} + R_n \\ J_n &= S_n \left(R_n^*\right)^{-1} \\ Q_n^* &= Q_n - S_n \left(R_n^*\right)^{-1} S_n^{\mathrm{T}} \\ \Phi_n^* &= \Phi_n - J_n H_n^*. \end{aligned}$$

The state prediction is obtained from the extended state space model of Eq. (15) as

$$\begin{aligned} \hat{x}_n^- &= \Phi_{n-1}^* \hat{x}_{n-1}^+ + J_{n-1} z_{n-1}^* \\ P_n^- &= \Phi_{n-1}^* P_{n-1}^+ \Phi_{n-1}^{*\mathrm{T}} + Q_{n-1}^*, \end{aligned} \tag{20}$$

and its update is given by

$$\begin{aligned} \hat{x}_n^+ &= \hat{x}_n^- + K_n \left(z_n^* - H_n^* \hat{x}_n^-\right) \\ P_n^+ &= \left(I - K_n H_n^*\right) P_n^-, \end{aligned} \tag{21}$$

with the Kalman gain

$$K_n = P_n^- H_n^{*\mathrm{T}} \left(H_n^* P_n^- H_n^{*\mathrm{T}} + R_n^* \right)^{-1}. \quad (22)$$

In the following subsections, this generalized Kalman filter is applied to pre-processed measurements, i.e. some a priori knowledge about the receiver and satellite positions (given by navigation message), satellite clock offsets, and tropospheric delays is subtracted from the original phase and code measurements. This means that only the errors in the geometry have to be estimated, which show much lower dynamics. This enables a much stronger state space model and, thereby, more accurate estimates of the orbital errors, receiver clock offsets, and satellite code biases. For simplicity, the tildes on all variables are omitted in Eq. (23), which describes the difference between original measurements and a priori knowledge:

$$\begin{aligned}
\lambda_1 \Delta\phi_{1,i}^k(t_n) &= \Delta g_i^k(t_n) - I_{1,i}^k(t_n) + \lambda_1 N_{1,i}^k + \\
&\quad \beta_{1,i} + \beta_1^k + \epsilon_{1,i}^k(t_n) \\
\lambda_2 \Delta\phi_{2,i}^k(t_n) &= \Delta g_i^k(t_n) - q_{12}^2 I_{1,i}^k(t_n) + \lambda_2 N_{2,i}^k + \\
&\quad \beta_{2,i} + \beta_2^k + \epsilon_{2,i}^k(t_n) \\
\Delta\rho_{1,i}^k(t_n) &= \Delta g_i^k(t_n) + I_{1,i}^k(t_n) + \eta_{1,i}^k(t_n) \\
\Delta\rho_{2,i}^k(t_n) &= \Delta g_i^k(t_n) + q_{12}^2 I_{1,i}^k(t_n) + \eta_{2,i}^k(t_n). \quad (23)
\end{aligned}$$

The geometry term can be further modeled as

$$\Delta g_i^k(t_n) = (\vec{e}_i^{\,k})^{\mathrm{T}} \Delta\, \vec{r}^{\,k}(t_n) + c\delta\tau_i + b_g^k, \quad (24)$$

where $\vec{e}_i^{\,k}$ denotes the unit vector from satellite to receiver, $\Delta\vec{r}^{\,k}$ denotes the satellite orbit correction, $c\delta\tau$ denotes the receiver clock/bias term, and b_g^k denotes the satellite code bias. A cascaded Kalman filter has the advantage that it enables a faster ambiguity resolution compared to an estimation of all unknowns in one single step, while it also reduces the computational complexity due to order reduction. However, the cascading of filters introduces time correlation into the a posteriori estimates, such that the assumption of white Gaussian measurement noise is no longer fulfilled for all filters except the first one. Therefore, the method of Bryson et al. shall be used to decouple the filters.

In the following section, an upper index (1) and (2) is introduced to well distinguish the variables between both Kalman filters when needed.

First stage: Phase bias estimation

The state vector of the first Kalman filter is written as

$$x_n^{(1)} = \left(\Delta g_n^{\mathrm{T}}, \Delta\dot{g}_n^{\mathrm{T}}, I_n^{\mathrm{T}}, \dot{I}_n^{\mathrm{T}}, \beta_R^{\mathrm{T}}, {\beta^K}^{\mathrm{T}}, N^{\mathrm{T}} \right)^{\mathrm{T}}, \quad (25)$$

where each element on the right side is itself a vector containing the elements for all links $i \to k$. The measurement vector combines two epochs of the phase and code measurements to allow a better estimation of the first derivatives of the geometry and ionospheric terms, i.e.

$$\begin{aligned}
z_n^{(1)} = \big(&\lambda_1 \varphi_{1,n}^{\mathrm{T}}, \lambda_2 \varphi_{2,n}^{\mathrm{T}}, \rho_{1,n}^{\mathrm{T}}, \rho_{2,n}^{\mathrm{T}}, \\
&\lambda_1 \varphi_{1,n+1}^{\mathrm{T}}, \lambda_2 \varphi_{2,n+1}^{\mathrm{T}}, \rho_{1,n+1}^{\mathrm{T}}, \rho_{2,n+1}^{\mathrm{T}} \big)^{\mathrm{T}}. \quad (26)
\end{aligned}$$

In the simulations, the standard deviations of the measurement noises are chosen to be

$$\begin{array}{lll}
\sigma_\phi = 5\ \mathrm{mm} & : & \text{phase noise} \\
\sigma_{\rho_{E1}} = 11.14\ \mathrm{cm} & : & \text{E1 code noise} \\
\sigma_{\rho_{E5}} = 1.93\ \mathrm{cm} & : & \text{E5 code noise,}
\end{array} \quad (27)$$

where the latter two values correspond to the Cramer Rao bound for a carrier to noise power ratio of 45 dB-Hz, a bandwidth of 20 MHz for the L1 CBOC signal and of 50 MHz for the E5 AltBOC signal. The state space covariance matrix of range and range-rate or ionospheric delay and its drift was derived by Brown et al. in [12] and is given by

$$\mathbf{\Sigma}_{\mathrm{w},\alpha\dot{\alpha}} = S_p \cdot \begin{pmatrix} \Delta t^4/4 & \Delta t^3/2 \\ \Delta t^3/2 & \Delta t^2 \end{pmatrix} \otimes \mathbf{1}^{s\times s}, \quad (28)$$

with s being the total number of links between visible satellites and receivers, and variable α being either Δg or I. There is in general no correlation between geometry, ionosphere and ambiguities, such that

$$\mathbf{\Sigma}_{\mathrm{w}} = \begin{pmatrix} \mathbf{\Sigma}_{\mathrm{w},\Delta g\Delta\dot{g}} & & \\ & \mathbf{\Sigma}_{\mathrm{w},I\dot{I}} & \\ & & \mathbf{\Sigma}_{\mathrm{w},N\beta} \end{pmatrix}, \quad (29)$$

with

$$\mathbf{\Sigma}_{\mathrm{w},b} = \mathbf{0}^{2s\times 2s}, \quad (30)$$

which means no process noise is assumed for the phase biases and the integer ambiguities. The spectral amplitudes of the random walk processes have been set to $S_p = 1\ \mathrm{mm}$ for the range rate, and $S_p = 1\ \mathrm{cm}$ for the ionospheric drift.

Second stage: Code bias estimation

The measurement vector of the second stage is set to the a posteriori state estimate of the first Kalman filter, i.e.

$$z_n^{(2)} = \hat{x}_n^{+,(1)}, \quad (31)$$

where the indices $+$ and $-$ denote the a posteriori and a priori estimates. In order to perform the filtering of the second stage, the matrix Γ_n in Eq. (5) representing the time correlation of the measurement noise, as well as the matrix R_n in Eq. (6) representing the covariance matrix of ζ_n, have to be determined. To simplify notations, all matrices except Γ_n are referring to the first Kalman filter.

The temporal correlation of the a posteriori state estimate of the first Kalman filter, which also equals the temporal correlation of the measurements of the second Kalman filter, is calculated as

$$E\left\{\left(\hat{x}_n^{+(1)} - E\{\hat{x}_n^{+,(1)}\}\right)\left(\hat{x}_{n-1}^{+,(1)} - E\{\hat{x}_{n-1}^{+,(1)}\}\right)^{\mathrm{T}}\right\}$$
$$= E\{(z_n^{(2)} - E\{z_n^{(2)}\})(z_{n-1}^{(2)} - E\{z_{n-1}^{(2)}\})^{\mathrm{T}}\}$$
$$= E\{v_n^{(2)} v_{n-1}^{(2)\mathrm{T}}\}. \quad (32)$$

This temporal correlation of the measurement noise is further developed with Eq. (5), i.e.

$$E\{v_n^{(2)} v_{n-1}^{(2),\mathrm{T}}\} = E\{(\Gamma_{n-1} v_{n-1}^{(2)} + \zeta_{n-1}) v_{n-1}^{(2),\mathrm{T}}\}$$
$$= \Gamma_{n-1} \cdot E\{v_{n-1}^{(2)} v_{n-1}^{(2),\mathrm{T}}\}. \quad (33)$$

Since

$$\hat{x}_n^{+,(1)} - x_n^{(1)} = \hat{x}_n^{-,(1)} + K_n \cdot (z_n^{(1)} - H_n \hat{x}_n^{-,(1)}) - x_n^{(1)}$$
$$= \Phi_{n-1}\hat{x}_{n-1}^{+,(1)} + K_n \cdot (z_n^{(1)} - H_n \Phi_{n-1}\hat{x}_{n-1}^{+,(1)}) - x_n^{(1)}$$
$$= (I - K_n H_n)\Phi_{n-1}\hat{x}_{n-1}^{+,(1)} + K_n (H_n x_n^{(1)} + v_n^{(1)}) - x_n^{(1)}$$
$$= (I - K_n H_n)\Phi_{n-1}\hat{x}_{n-1}^{+,(1)} -$$
$$(I - K_n H_n)(\Phi_{n-1} x_{n-1}^{(1)} + w_{n-1}^{(1)}) + K_n v_n^{(1)}$$
$$= (I - K_n H_n)\Phi_{n-1}(\hat{x}_{n-1}^{+,(1)} - x_{n-1}^{(1)}) +$$
$$(I - K_n H_n) w_{n-1}^{(1)} + K_n v_n^{(1)}, \quad (34)$$

and there is no cross-correlation between the a posteriori state estimate $\hat{x}_{n-1}^{+,(1)}$ and the true noise w_{n-1} and v_n, another way to calculate the temporal correlation of the a posteriori estimates of the first Kalman filter is given by

$$E\left\{\left(\hat{x}_n^{+(1)} - E\{\hat{x}_n^{+,(1)}\}\right)\left(\hat{x}_{n-1}^{+,(1)} - E\{\hat{x}_{n-1}^{+,(1)}\}\right)^{\mathrm{T}}\right\}$$
$$= (I - K_n H_n)\Phi_{n-1} P_{n-1}^{-} \quad (35)$$

Combining Eq. (32), (33), and (35) yields the matrix Γ_{n-1}:

$$\Gamma_{n-1} = (I - K_n H_n)\Phi_{n-1} \quad (36)$$

The covariance matrix R_{n-1} can be derived by

$$R_{n-1} = \mathbb{E}\{\zeta_{n-1}\zeta_{n-1}^{\mathrm{T}}\}$$
$$= \mathbb{E}\{(v_n - \Gamma_{n-1} v_{n-1})(v_n - \Gamma_{n-1} v_{n-1})^{\mathrm{T}}\}$$
$$= \mathbb{E}\{v_n v_n^{\mathrm{T}}\} - \Gamma_{n-1}\mathbb{E}\{v_{n-1} v_n^{\mathrm{T}}\} - \mathbb{E}\{v_n v_{n-1}^{\mathrm{T}}\}\Gamma_{n-1}^{\mathrm{T}}$$
$$+ \Gamma_{n-1}\mathbb{E}\{v_{n-1} v_{n-1}^{\mathrm{T}}\}\Gamma_{n-1}^{\mathrm{T}}. \quad (37)$$

Applying Eq. (33), it can be further simplified to

$$R_{n-1} = \mathbb{E}\{v_n v_n^{\mathrm{T}}\} - \Gamma_{n-1}\mathbb{E}\{v_{n-1} v_{n-1}^{\mathrm{T}}\}\Gamma_{n-1}^{\mathrm{T}}$$
$$= P_n^{+} - \Gamma_{n-1} P_{n-1}^{+} \Gamma_{n-1}^{\mathrm{T}}. \quad (38)$$

According to Eq. (24), the state vector of the second Kalman filter is defined as

$$x^{(2)} = \left(\Delta\vec{r}^{K,\mathrm{T}}, \Delta\dot{\vec{r}}^{K,\mathrm{T}}, c\delta\tau_R^{\mathrm{T}}, b_{g^K}^{\mathrm{T}}\right)^{\mathrm{T}}, \quad (39)$$

where the orbital error has a linear dynamic state model:

$$\Delta\vec{r}_n^{K} = \Delta\vec{r}_{n-1}^{K} + \Delta t \Delta\dot{\vec{r}}_{n-1}^{K} + w_{\Delta\vec{r}_{n-1}^{K}}. \quad (40)$$

Since the radial component of the orbital error is the most difficult term to estimate within short time, it is necessary to separate the radial direction from the Earth-Centered Earth-Fixed (ECEF) unit vector. Therefore, the satellite local Radial, In- and Cross-track (RIC) coordinate frame is used. The transformation from RIC to ECEF is given by

$$\begin{pmatrix} \Delta r_{\mathrm{x}} \\ \Delta r_{\mathrm{y}} \\ \Delta r_{\mathrm{z}} \end{pmatrix} = R_{\mathrm{z}}(\theta) \cdot \begin{pmatrix} \vec{e}_{\mathrm{R}}^{\mathrm{T}} \\ \vec{e}_{\mathrm{I}}^{\mathrm{T}} \\ \vec{e}_{\mathrm{C}}^{\mathrm{T}} \end{pmatrix} \cdot \begin{pmatrix} \Delta r_{\mathrm{R}} \\ \Delta r_{\mathrm{I}} \\ \Delta r_{\mathrm{C}} \end{pmatrix}, \quad (41)$$

where matrix R_{z} describes the rotation counter-clockwise through an angle θ from Earth-Centered Inertial (ECI) frame to ECEF frame along the earth rotation axis, which points towards the observer, and the vectors $\vec{e}_{\mathrm{R}}$, $\vec{e}_{\mathrm{I}}$ and $\vec{e}_{\mathrm{C}}$ represent respectively the unit vectors in radial, in- and cross-track directions. Given the position vector $\vec{r}_{\mathrm{ECI}}$ in ECI frame, the direction of $\vec{e}_{\mathrm{R}}$ coincides with the position direction, the cross-track unit vector $\vec{e}_{\mathrm{C}}$ lies along the angular momentum vector $\vec{L} = \vec{r}_{\mathrm{ECI}} \wedge \dot{\vec{r}}_{\mathrm{ECI}}$, and the in-track vector completes the right-hand system [13].

In the simulation, the states including Eq. (25) and (39) are generated in one step based on 20 globally distributed IGS (International GPS Service) stations. The generated satellite orbital corrections consist of the in- and cross-track components, while the radial component is assumed to be known perfectly. A cascaded Kalman filter has been implemented to estimate all states: In the first stage, the ionospheric slant delays, the integer ambiguities, the phase biases as well as the geometry terms are estimated.

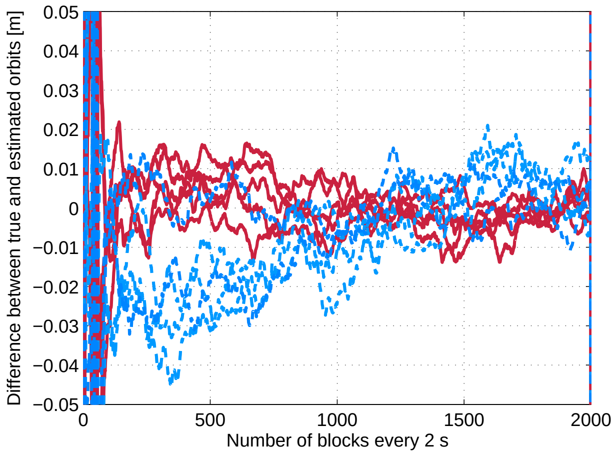

Fig. 6 The difference between the true satellite in-, cross-track corrections and the estimates.

The geometry estimates, whose noise is sequentially correlated, are then used as measurements for estimating the satellite in- and cross-track corrections, the receiver clock/bias terms and the satellite code biases in the second stage. Fig. 6 shows difference between the true orbital corrections and the estimates. The error in the estimates converges to under 2 cm after 700 epochs. Fig. 7 shows the error in the satellite code bias estimates. After 500 epochs the estimates have reached a level of 1 cm.

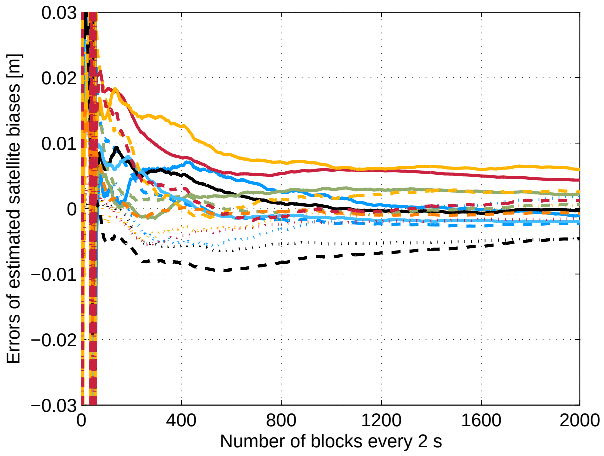

Fig. 7 The error between generated satellite code biases and the estimates.

CONCLUSION

In this work, the code multipath analysis as well as the code bias estimation have been performed. Given a network of ground stations from SAPOS, a daily multipath pattern has been observed in the code residuals. A sidereal filtering has been applied to the samples gathered over one week, such that the multipath pattern could be isolated and removed from the measurements. The effect on real data was an almost complete mitigation of the multipath, resulting in an almost white noise and in a much better ambiguity fixing behavior. In the second section, a cascaded Kalman filter has been proposed for the efficient estimation of satellite phase and code biases. The time-correlation introduced by the first Kalman filter has been taken into account by Bryson's generalized Kalman filter for colored measurement noise. The simulation results show that the difference between the estimated orbital errors and the true ones has been converged to less than 2 cm within 23 min, and the difference between satellite code bias estimates and the true ones has dropped below 1 cm after 17 min.

ACKNOWLEDGEMENT

The authors would like to thank the German Federal Ministry of Economics and Technology and the German Aerospace Center (DLR) for a financial grant to the project MIMGAL (FKZ: 50NA0911) that supported this work. The authors would also like to thank the Bavarian Landesamt für Vermessung und Geoinformation for the free access to SAPOS measurements.

REFERENCES

[1] Z. Wen, P. Henkel, and C. Günther, Reliable estimation of phase biases of GPS satellites with a local reference network. *Proc. of 53rd IEEE Intern. Symposium ELMAR*, Zadar, Croatia, pp. 321-324, Sept. 2011.

[2] P. Henkel, Z. Wen, and C. Günther, Estimation of satellite and receiver biases on multiple galileo frequencies with a Kalman filter. *Proc. of ION Int. Techn. Meeting*, San Diego, USA, pp. 1067-1074, 2010.

[3] Z. Wen, Estimation of Code and Phase Biases in Satellite Navigation. *Master thesis*, Technische Universität München, 2010.

[4] M. Davaine, Code bias estimation and multipath estimation with cascaded Kalman filter. *Master Thesis*, Munich, 2011.

[5] D. Laurichesse, F. Mercier, Integer ambiguity resolution on undifferenced gps phase measurements and its application to ppp. *Proc. of ION-GNSS*, Forth Worth, USA, pp. 839-848, Sept. 2007.

[6] D. Laurichesse, F. Mercier, J.-P. Berthias, P. Brocca, and L. Cerri, Integer ambiguity resolution on undifferenced gps phase measurements and its application to ppp and satellite precise orbit determination. *Navigation*, vol. 56, no. 2, pp. 135-149, 2009.

[7] D. Laurichesse, F. Mercier, J.-P. Berthias, Real-time ppp with undifferenced integer ambiguity resolution, experimental results. *Proc. of 23rd ION Intern. Techn. Meet. (ION-GNSS)*, pp. 2534-2544, Sep. 2010.

[8] G. Wübbena, GPS carrier phases and clock modeling. *Lecture Notes in Earth Sciences: GPS-Techniques Applied to Geodesy and Surveying*, vol. 19, pp. 381-392, 1988.

[9] A. E. Bryson, Jr. and L. J. Henrikson, Estimation using sampled-data containing sequentially correlated noise. *J. of Spacecraft and Rockets*, 5(6), 662-665, 1968.

[10] K. Wang, Y. Li, and C. Rizos, New practical approach to Kalman filtering with time-correlated measurement errors. 2010.

[11] Sapos Bayern - Referenzstationen, Bayerische Vermessungsverwaltung. *http://sapos.bayern.de*, accessed on Jun. 7, 2011.

[12] R. Brown and P. Hwang, Introduction to random signals and applied Kalman filtering, 3rd edition. John Wiley & Sons, New York, 1997.

[13] G. Born, Introduction to statistical orbit determination. *Lecture notes*, University of Colorado, 2011.